Journal of Inorganic and General Chemistry
ZAAC
Zeitschrift für anorganische und allgemeine Chemie
www.zaac.wiley-vch.de
RESEARCH ARTICLE

DOI: 10.1002/zaac.202200219

Facile Synthesis and Characterization of Pure Tochilinite-like Materials from Nanoparticulate FeS

Robert Bolney,[a] Mario Grosch,[a] Mario Winkler,[b] Joris van Slageren,[b] Wolfgang Weigand,*[a] and Christian Robl*[a]

Dedicated to Professor Dr. Thomas Schleid on the occasion of his 65th Birthday.

In this work, three different tochilinite-like materials have been obtained by sophisticated synthetic methods that allow to control the distribution of iron ions. The purity of the samples was confirmed by powder X-ray diffraction. From elemental analysis and Mössbauer spectroscopy data, detailed compositions could be determined: T1) $Fe_{0.76}S$*0.86 $[Fe^{2+}_{0.01}Fe^{3+}_{0.56}Mg^{2+}_{0.43}(OH)_{2.01}]$; T2) $Fe_{0.89}S$*0.85 $[Fe^{2+}_{0.55}Fe^{3+}_{0.11}Al^{3+}_{0.33}(OH)_{1.84}(O)_{0.16}]$; T3) $Fe_{0.71}S$*0.79 $[Fe^{2+}_{0.25}Fe^{3+}_{0.73}Mg^{2+}_{0.01}Al^{3+}_{0.01}(OH)_{1.98}(O)_{0.02}]$. These compositions fit to typical compositions of tochilinite in regard of the amount of iron vacancies and the volume ratio of the hydroxide layers to the sulfide layers. Besides hydroxide ions, oxide ions are also present in the hydroxide layers as a result of surface oxidation after the synthesis due to the high reactivity of the particles. TEM and SEM investigations show that the obtained powders consist mainly of thin sheets accompanied by nanotubes with BET surface areas ranging between 20 m^2/g and 40 m^2/g. The thermal stability was investigated by TGA and DSC analysis and it depends significantly on the composition.

Introduction

Tochilinite (Figure 1) is a rare layered hybrid mineral that belongs to the valleriite mineral group. This group contains all known hybrid minerals that are composed of sulfide and hydroxide layers. Tochilinite consists of iron sulfide and magnesium hydroxide layers with slightly distorted mackinawite and brucite structures as described by Organova *et al.* in 1973. Tochilinite has been reported to crystallize in the space group P1 with triclinic symmetry but monoclinic metrics with a = 5.37 Å, b = 15.65 Å, c = 10.72 Å; $\alpha = \beta = 90°$ and $\gamma = 95°$. Tochilinite is mainly found in carbonaceous chondrites and rarely occurs at sulfide ore deposits.[2–6] As tochilinite is a rarely occurring mineral, a convenient synthesis for pure tochilinite is required. Layered hybrid materials have attracted some attention as functional materials for electronic, magnetic and optical applications and tunable tochilinite may be an interesting candidate for future developments.[7–11] Additionally, it may be a suitable mediator for prebiotically relevant reactions as has been suggested and experimentally shown for other iron sulfides.[12–16] Besides being delivered by meteoritic impacts, tochilinite forms from iron sulfides in basic anoxic environments and might have been quite common on the early earth.[17,18] Synthetic tochilinite has been produced before, however, without the ability to control the iron ion distribution and the samples have always been contaminated by side products like pyrrhotite, pyrite and magnetite.[19–22] Therefore, a compositional analysis of the sulfide and the hydroxide layers independent of each other has not been reported so far. Previous studies were limited to diffraction experiments or Mössbauer studies.[4,19–26] This work is the first to report on a synthesis of pure tochilinite-like materials. The combination of X-ray diffraction, Mössbauer spectroscopy and elemental analysis by ICP-OES made it possible to obtain detailed compositions of the synthetic materials.

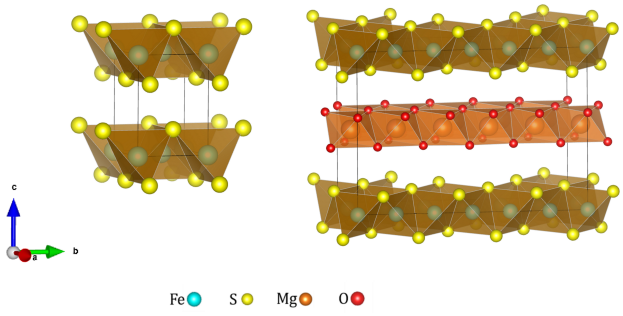

Figure 1. Unit cells of mackinawite[1] (left) and tochilinite[2] (right).

[a] *Dr. R. Bolney, Dr. M. Grosch, Prof. Dr. W. Weigand, Prof. Dr. C. Robl*
Faculty of Chemistry and Earth Sciences, Institute of Inorganic and Analytical Chemistry, Friedrich Schiller University Jena, Humboldtstrasse 8, 07743 Jena, Germany
Tel: +49 36419-48160
E-mail: christian.robl@uni-jena.de
wolfgang.weigand@uni-jena.de
[b] *M. Winkler, Prof. Dr. J. van Slageren*
Institute of Physical Chemistry, University of Stuttgart, Pfaffenwaldring 55, 70569 Stuttgart, Germany

Supporting information for this article is available on the WWW under https://doi.org/10.1002/zaac.202200219

Results and Discussion

Natural tochilinite contains Fe^{2+} in the sulfide layers and mainly Mg^{2+}, Al^{3+}, Fe^{2+} and Fe^{3+} in the hydroxide layers with a composition of

$$Fe^{2+}{}_{1-x}\ S\ ^{*}\ y\ [Fe^{2+}{}_{a}Fe^{3+}{}_{b}Mg^{2+}{}_{c}Al^{3+}{}_{d}\ (OH)_2] \text{ with}$$
$$0.1 < x < 0.3 \text{ and } a + b + c + d = 1 \text{ and } b + d = x$$
$$\text{and } 0.7 < y < 0.9$$[2,3,5,22,27–29]

Our aim was to synthesize tochilinite-like materials with three different compositions of:

T1) $Fe^{2+}{}_{1-x}\ S\ ^{*}\ y\ [Fe^{3+}{}_{x}Mg^{2+}{}_{1-x}(OH)_2]$

T2) $Fe^{2+}{}_{1-x}\ S\ ^{*}\ y\ [Fe^{2+}{}_{1-x}\ Al^{3+}{}_{x}\ (OH)_2]$

T3) $Fe^{2+}{}_{1-x}\ S\ ^{*}\ y\ [Fe^{2+}{}_{1-x}Fe^{3+}{}_{x}(OH)_2]$

with $0.1 < x < 0.3$ and $0.7 < y < 0.9$.

As has been described before, we used a hydrothermal synthesis approach.[4,17,21,22] In contrast to previous works, we only used solid Fe, S, Al, Mg and FeO(OH) without any soluble salts. One advantage of using elemental metals is that their oxidation provides a sufficiently high hydrogen gas pressure that is necessary to limit the oxidation of Fe^{2+} to Fe^{3+}. All syntheses were carried out in stainless-steel pressure reactors with a Teflon inlet. The side products that needed to be dealt with are pyrrhotite, pyrite, magnetite and residual iron.

Synthesis of T1, magnesium tochilinite

For the synthesis of T1, a two-step procedure was developed. At first, a suspension of FeS nanoparticles in water was synthesized from an equimolar amount of elemental sulfur and elemental iron following the procedure as described previously by us.[18] Then, a suspension of powdered magnesium and FeO(OH) was prepared in a stainless-steel pressure reactor with a Teflon inlet. Both suspensions were combined and heated under autogenous pressure for 3 days at 160 °C. Pyrrhotite and pyrite formation could be suppressed by using the two-step process and an excess of FeO(OH). Magnesium in contact with elemental sulfur and water oxidizes very fast and forms soluble magnesium polysulfides. The S^{2-} and Fe^{2+} released by FeS dissolution rapidly react with dissolved FeO(OH) and Mg^{2+} to form tochilinite. Excess Mg^{2+}, Fe^{2+} and Fe^{3+} precipitate as Mg^{2+}-containing magnetite that is the least soluble compound in this system. Residual elemental iron and any magnetite can be removed after the reaction with a strong magnet leading to pure magnesium tochilinite samples.

Synthesis of T2, aluminum tochilinite

The aluminum tochilinite we aimed at should only contain Al^{3+} and Fe^{2+} in the hydroxide layers. To suppress the formation of Fe^{3+} in the reaction solution, a relatively high hydrogen gas pressure was maintained during the reaction. This was done by a comparable high total mass of the starting materials. A suspension of a finely ground mixture of Fe, S and Al in water was prepared and heated for 3 days at 130 °C. Pyrrhotite and pyrite formation could be suppressed by the kinetic control of the reaction and an excess of elemental iron. As aluminum very rapidly oxidizes in hot water, the Al^{3+} availability is high already at the beginning of the reaction.

$$2\ Al + 6\ H_2O \rightarrow 2\ Al(OH)_3 + 3\ H_2\ \uparrow \quad (1)$$

The high H_2-pressure arising from this reaction slows the oxidation of Fe in a way, that it mainly oxidizes in the reaction with elemental sulfur.

$$Fe + 2\ H_2O \rightarrow Fe(OH)_2 + H_2\ \uparrow \quad (2)$$

$$Fe + S \rightarrow FeS \quad (3)$$

The so formed FeS rapidly reacts with Al^{3+} and OH^- to form stable tochilinite crystallites giving the FeS little time to convert to pyrrhotite ($Fe_{1-x}S$) or to form pyrite (FeS_2). The excess elemental iron and any magnetite formed was again removed after the reaction using a strong magnet leading to pure aluminum tochilinite samples.

Synthesis of T3, ferrotochilinite

The tochilinite analogue containing only iron ions is called ferrotochilinite[29] and is easily available by the following method. An aqueous suspension of a finely ground mixture of elemental iron and sulfur in a 3:1 mass ratio that is heated at 130 °C for three days already leads to its formation. Pyrrhotite and pyrite formation could be suppressed by using an excess of elemental iron. The oxidation of the elemental iron in this system is fast enough to provide the necessary amounts of Fe^{2+}, Fe^{3+} and OH^- to rapidly form stable tochilinite particles that do not transform significantly to pyrrhotite at the reaction temperature. If the suspension of iron and sulfur is heated at 160 °C instead of 130 °C, only magnetite and pyrrhotite are formed. The excess elemental iron and any magnetite formed was again removed after the reaction using a strong magnet leading to pure ferrotochilinite samples.

Powder X-Ray Diffraction

Typical XRD patterns for the three tochilinite analogues are shown in Figures S1 to S3. The XRD patterns are dominated by two strong reflections, the d-values of which at approximately 11 Å and 5.5 Å can be assigned to the 001 and 002 diffraction

peaks as previously reported for natural tochilinite.[2,3,17] All other diffraction peaks have little intensity, which might by caused by preferred orientation or turbostratic stacking of the layers. From the obtained patterns it can be concluded, that none of the known side products of pyrrhotite, pyrite, magnetite and residual iron are present in significant amounts after the work up procedure.

Elemental Analysis by ICP-OES

Elemental analyses of the tochilinite samples were carried out by ICP-OES and the obtained compositions are shown in Table 1, 2.

Mössbauer spectroscopy

Mössbauer spectroscopy was used to discriminate between the different iron species that can be expected from previous works on tochilinite (Table 2). The room temperature spectra are given in Figures S4 to S6 and the fit parameters are given in Tables TS2 to TS4. The Mössbauer data for T1 and T2 were obtained by fitting the Mössbauer spectrum for ^{57}Fe with three different iron species: Fe^{2+} in a tetrahedral sulfide environment (Fe^{2+}_S) as well as Fe^{2+} and Fe^{3+} in an octahedral hydroxide environment (Fe^{2+}_{H1}/Fe^{3+}_H). For the fit of T3, a second Fe^{2+} species in a slightly different octahedral hydroxide environment (Fe^{2+}_{H2}) was introduced in accordance with previous reports.[23] All signals are split into two lines by quadrupole splitting. For synthetic mackinawite an isomer shift of 0.37 mms^{-1} was found at room temperature.[18,30] The slightly higher isomer shifts (0.41 mms^{-1} to 0.45 mms^{-1}) obtained for the Fe^{2+} in the mackinawite-like layers in tochilinite compared to those in pure mackinawite might arise from an expansion of the unit cell[23,24] or the iron deficiency that leads to different Fe–S distances, thereby influencing the isomer shift.[2] The quadrupole splitting of the signals is very small with 0.18 to 0.24 $mm\,s^{-1}$.

The determined values of $Fe^{2+}_{(S)}$, $Fe^{2}_{(H1)}$ and $Fe^{2+}_{(H2)}$ (Table 2) fit well to literature values for tochilinite and the values for $Fe^{3+}_{(H)}$ to the structurally similar valleriite as is shown in Table TS1.

The fitted areas for $Fe^{2+}_{(S)}$ and $Fe^{3+}_{(H)}$ strongly overlap and are partly interchangeable without lowering the quality of the fit. Therefore, reasonable constraints were applied to the fit of $Fe^{2+}_{(S)}$. Regarding the sulfur content obtained from ICP-OES, the content of $Fe^{2+}_{(S)}$ cannot have arbitrary values. It has been reported multiple times, that tochilinite contains less $Fe^{2+}_{(S)}$ compared to the amount of sulfide ions. As these iron vacancies in mackinawite-like layers have not been reported to be more than 30%,[4,5,31,19–26] a minimum and a maximum value for $Fe^{2+}_{(S)}$ was given for the fit. The ranges of error for the proportions of $Fe^{2+}_{(S)}$ and $Fe^{3+}_{(H)}$ might therefore be higher than given.

The unassigned sample fractions (marked as n.d.) are assumed to represent the masses of H_2O, OH^- and O^{2-}. As the sulfur content is only expected in the form of sulfide ions, charge balancing was used to determine the amounts of OH^- and O^{2-}. Natural tochilinite is reported to only contain hydroxide ions. Therefore, the total residual mass was initially assumed to represent only hydroxide ions, but in the cases of T2 and T3 there were more positive than negative charges. To obtain balanced charges, some of the hydroxide ions were replaced by oxide ions. The resulting compositions are summarized in Table 3.

The occurrence of oxide instead of hydroxide ions is reasonable, as the data obtained from ICP-OES and Mössbauer spectroscopy were obtained from samples subjected to oxidation by air. In this regard, surface oxidation of Fe^{2+} to Fe^{3+} can easily lead to the formation of oxide ions. The surface oxidation of freshly prepared tochilinite-like materials following the synthesis routes described here, is very exothermic. The samples showed pyrophoric behavior and needed to be cooled during their first air contact. This was done by an additional stream of nitrogen gas while isolating and drying the solid materials by filtration. After the oxidation of the particle surfaces, the materials could be handled in air without the risk of ignition. The calculated formulas fit to typical composition of natural tochilinite in regard of the general composition but also the amount of iron vacancies and the volume ratio of hydroxide to sulfide layers. The compositional data clearly show that the controlled synthesis of tochilinite analogues was successful.

Table 1. Compositions obtained from ICP-OES.

	Fe/mg	S/mg	Mg/mg	Al/mg	n.d./mg *
T1	57.92 ±0.93	27.50 ±1.98	8.92 ±0.01	0.02 ±0.01	30.03 ±2.55
T2	58.25 ±0.93	22.92 ±1.65	0.00 ±0.01	5.32 ±0.06	28.99 ±2.67
T3	63.25 ±1.03	24.25 ±1.75	0.03 ±0.01	0.07 ±0.01	23.20 ±2.59

* n.d. = not determined. A portion of the analyzed sample masses cannot be assigned to Fe, S, Mg or Al and is assumed to represent the H and O content.

Table 2. Content of the different iron ions obtained by Mössbauer spectroscopy.

Compound	$Fe^{2+}_{(S)}$	$Fe^{2+}_{(H,1)}$	$Fe^{2+}_{(H2)}$	$Fe^{3+}_{(H)}$
T1	59 ± 5%	3 ± 3%	–	38 ± 5%
T2	55 ± 5%	32 ± 5%	–	13 ± 5%
T3	46 ± 5%	10 ± 3%	5 ± 3%	38 ± 5%

Table 3. Compositions obtained from combining ICP-OES and Mössbauer data compared to the composition reported by Organova *et al.*[2]

Compound	Composition*
T1	$Fe_{0.76}S*0.86\ [Fe^{2+}_{0.01}Fe^{3+}_{0.56}Mg^{2+}_{0.43}(OH)_{2.01}]$
T2	$Fe_{0.89}S*0.85\ [Fe^{2+}_{0.55}Fe^{3+}_{0.11}Al^{3+}_{0.33}(OH)_{1.84}(O)_{0.16}]$
T3	$Fe_{0.71}S*0.79$ $[Fe^{2+}_{0.25}Fe^{3+}_{0.73}Mg^{2+}_{0.01}Al^{3+}_{0.01}(OH)_{1.98}(O)_{0.02}]$
Natural Tochilinite[2]	$Fe_{0.9}S*0.83\ [Mg_{0.71}Fe_{0.29}(OH)_2]$

Tochilinite particle characteristics

All samples have been investigated by scanning electron microscopy (SEM) and transmission electron microscopy (TEM) (Figures 2–6). The SEM images show thin platelets and nanotubes as has been reported for natural and synthetic tochilinite.[17,22,32] The edge lengths of the thin platelets are in the micrometer regime but they are only nanometers thick.

The T1 and T2 samples are composed of platelets with various shapes whereas the T3 sample shows a more heterogenous picture probably due to oxidation. A sample of T1 was also investigated by TEM. The obtained images show an accumulation of nanotubes probably caused by the sample preparation. As the small particles form micrometer-sized aggregates which could hardly be separated, only the edges of these aggregates could be investigated.

BET surface areas were determined using adsorption isotherms of argon gas at 87 K. The determined surface areas are summarized in Table 4.

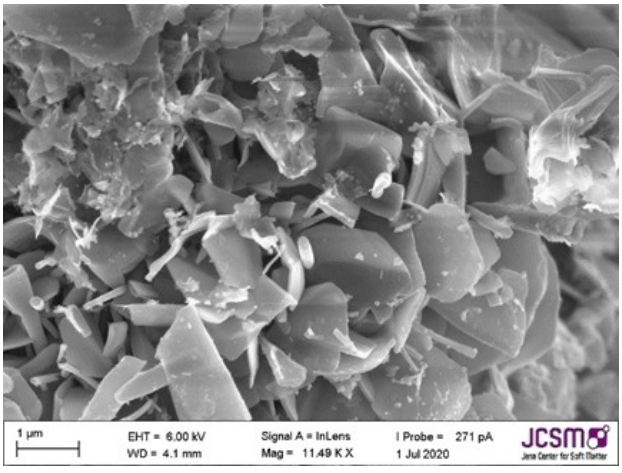

Figure 2. SEM image of T1.

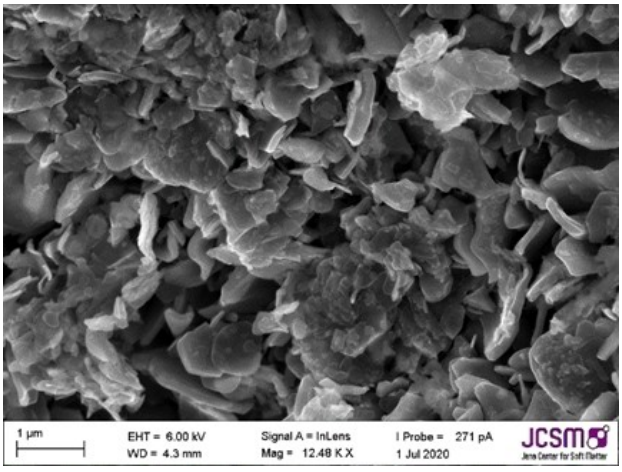

Figure 3. SEM image of T2.

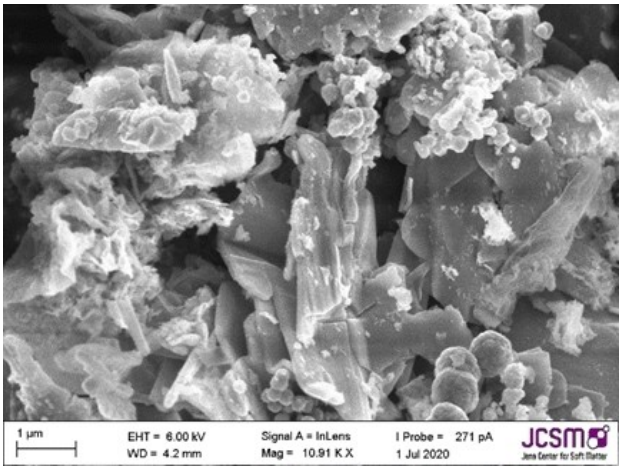

Figure 4. SEM image of T3.

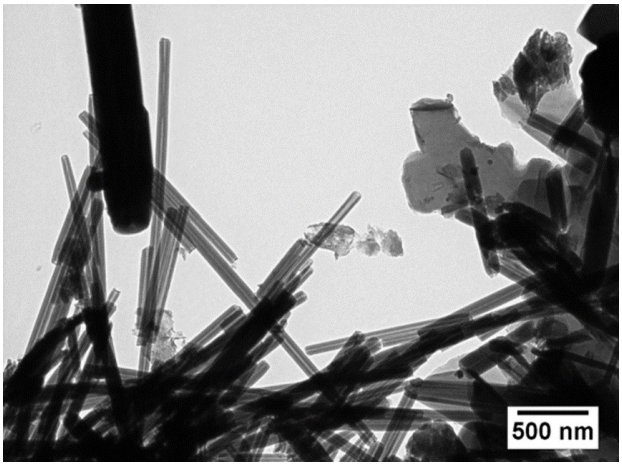

Figure 5. Magnified TEM image of T1.

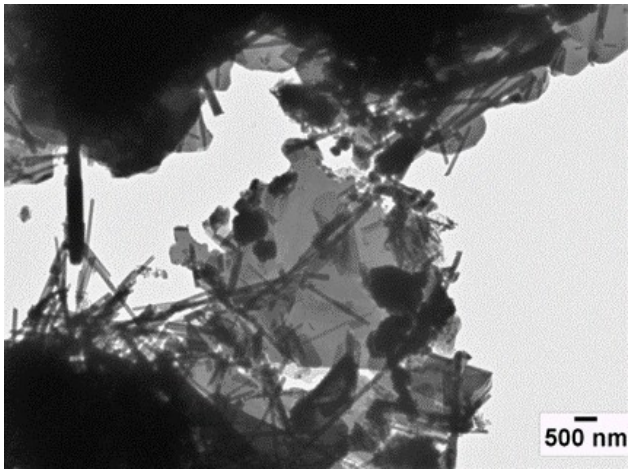

Figure 6. TEM image of T1.

Table 4. BET surface areas determined from argon adsorption isotherms.

Compound	BET surface area/m^2*g^{-1}
T1	40 ± 1
T2	31 ± 1
T3	23 ± 1

Thermogravimetry and Differential Scanning calorimetry

The TGA/DSC analyses show (Figures S7 to S9), that the mass of all samples decreases from the start already at low temperatures. This may be attributed to a loss of adsorbed water as the samples were used shortly after their synthesis without excessive drying. The pronounced loss of mass at higher temperatures is attributed to the formation of magnetite, magnesioferrite and pyrrhotite accompanied by the loss of water. The temperatures at which the decomposition starts is in the order T1 (335 °C) > T2 (318 °C) > T3 (243 °C). The stability of the tochilinite analogues clearly changes with their composition.

Conclusions

The synthesis of tochilinite has been described before but a proper characterization with an elemental analysis was missing. In this work, three different pure tochilinite analogues have been obtained by synthetic methods that allow to control the composition of the hydroxide layers. Moreover, the formation of any side product could either be suppressed or removed after the reaction. Ferrotochilinite containing exclusively Fe^{2+} and Fe^{3+} in the hydroxide layers has not been synthesized before.

T1) $Fe_{0.76}S * 0.86\ [Fe^{2+}_{0.01}Fe^{3+}_{0.56}Mg^{2+}_{0.43}(OH)_{2.01}]$

T2) $Fe_{0.89}S * 0.85\ [Fe^{2+}_{0.55}Fe^{3+}_{0.11}Al^{3+}_{0.33}(OH)_{1.84}(O)_{0.16}]$

T3) $Fe_{0.71}S * 0.79\ [Fe^{2+}_{0.25}Fe^{3+}_{0.73}Mg^{2+}_{0.01}Al^{3+}_{0.01}(OH)_{1.98}(O)_{0.02}]$

These formulas show that the compositions obtained fit to typical composition of natural tochilinite in regard of the general composition but also the amount of iron vacancies and the volume ratio of hydroxide to sulfide layers. The oxidation state of iron ions could be controlled within a small margin of error by using appropriate reaction conditions. Controlling the different ion concentrations by the kinetics of their release and consumption is a suitable approach to synthesize complex layered hybrid sulfide minerals. This may offer the exploration of synthetic analogues of other valleriite-group minerals like yushkinite, haapalaite vyalsovite, ekplexite and kaskasite. Additionally, the formation conditions described in these syntheses may offer a deeper insight into natural tochilinite formation in outer space as well as on the early earth.

Experimental Section

T1, magnesium tochilinite

88 g of a mixture of iron and sulfur with a molar ratio of 1:1. was ground thoroughly in an automated mortar. 3.00 g of this mixture containing powdered iron (1.904 g, 34 mmol) and powdered sulfur (1.096 g, 34 mmol) was transferred into a 25-ml microwave vial and sodium chloride (0.181 g, 3 mmol) was added. The vial was sealed and the air was replaced by nitrogen. To this mixture 10 ml of deaerated water was added and the resulting suspension was kept at room temperature overnight without stirring. The solids turned black within a couple of hours and the complete conversion to mackinawite was controlled with a strong magnet. In a steel autoclave with a Teflon inlet, powdered magnesium (0.36 g, 16 mmol) and powdered iron oxide hydroxide (0.30 g, 5 mmol) were mixed with the iron sulfide suspension and 10 ml of deionized water were added. The reactor was sealed and heated in an oven for 4 days at 160 °C without stirring. After cooling down to room temperature, the obtained black suspension was transferred into a 500 ml beaker and charged with 200 ml deionized water. The suspension was stirred with a strong magnet for multiple minutes and all magnetic material was removed. The residual solid was isolated by filtration, washed successively with water, ethanol, acetone and diethyl ether and dried under a stream of nitrogen gas.

T2, aluminum tochilinite

90.6 g of a mixture of iron, sulfur and aluminum was ground thoroughly in an automated mortar. 9.06 g of this mixture containing powdered iron (6.000 g, 107 mmol), powdered sulfur (2.460 g, 77 mmol) and powdered aluminum (0.600 g, 22 mmol) were transferred into a steel autoclave with a Teflon inlet. 20 ml of deionized water were added and the reactor was sealed and heated in an oven for 3 days at 130 °C without stirring. After cooling down to room temperature, the obtained black suspension was transferred into a 500 ml beaker and stirred with a strong magnet for 5 minutes and all magnetic solids were removed. The solid was isolated by filtration and washed successively with water, ethanol, acetone and diethyl ether and dried under a stream of nitrogen gas.

T3, ferrotochilinite

40 g of a mixture of iron and sulfur was ground thoroughly in an automated mortar. 4.00 g of this mixture containing powdered iron (3.000 g, 54 mmol) and powdered sulfur (1.000 g, 31 mmol) and additional powdered sulfur (0.111 g, 3 mmol) were transferred into a steel autoclave with a Teflon inlet and 20 ml of deionized water were added. The reactor was sealed and heated in an oven for 3 days at 130 °C without stirring. After cooling down to room temperature, the obtained black suspension was transferred into a 500 ml beaker and stirred with a strong magnet for 5 minutes and all magnetic solids were removed. The solid was isolated by filtration and washed successively with water, ethanol, acetone and diethyl ether and dried under a stream of nitrogen gas.

Powder X-ray diffraction (XRD)

Powder X-ray diffraction (XRD) patterns were collected at a tabletop Rigaku Mini-Flex 600 equipped with a copper anode with 0.6 kW and an energy dispersive detector to minimize effects of X-ray fluorescence.

Elemental Analysis by ICP-OES

Elemental analysis was carried out with an ICP-OES spectrometer 725ES (Agilent, Waldbronn, Germany) with CCD-detector. The samples were dissolved in aqua regia in acid digestion vessels at high temperatures. The vessels used could not be charged with the tochilinite sample and the acids without the loss of H_2S before they can be closed. To circumvent this problem, the samples were loaded into the digestion vessels and charged with 10 ml of water to cover the sample completely. The water was frozen carefully with liquid nitrogen so that the tochilinite sample was protected by a cover of ice. On top of the ice surface, 10 ml of aqua regia was added and the autoclave sealed before the ice starts to melt. The autoclaves were then heated to 130 °C overnight to obtain clear and deep orange solutions. The solutions were transferred into a 250 ml volumetric flask and filled to the mark with distilled water. The obtained solutions were immediately transferred into polyethylene vials to reduce any contamination from the glass walls and subjected to ICP-OES analysis.

Mössbauer spectroscopy

Mössbauer spectra were obtained on a homemade spectrometer based on a RCPTM MS-96 Mössbauer spectrometer equipped with a Ritverc Co57 in a Rh-matrix source, a YAP:Ce scintillating crystal detector, and a Janis SVT-400 helium-bath cryostat. The samples (roughly 30 mg) were filled into weighing paper that was folded to squares, and parafilm was wrapped tightly around it. The sample was inserted into an Al sample holder, which was then inserted into the Mössbauer spectrometer. Spectra were calibrated against α-iron at room temperature and fitted using the MossWinn 4.01 software.

SEM and TEM imaging

Scanning electron microscopy (SEM), High-resolution transmission electron microscopy (TEM) and BET-analysis were used to investigate the tochilinite particle characteristics. SEM imaging was performed with a Sigma VP Field Emission Scanning Electron Microscope (Carl-Zeiss AG, Germany) using the InLens detector with an accelerating voltage of 6 kV. EDX was performed with an Oxford EDX system in combination with a Sigma VP Field Emission Scanning Electron Microscope (Carl-Zeiss AG, Germany). TEM measurements were conducted with a FEI Tecnai G^2 20 Transmission Electron Microscope. 15 µL of the sample solution was blotted onto lacey carbon grids (Plano). Images were acquired at an acceleration voltage of 200 kV.

BET surface areas

BET surface areas of tochilinite were determined with a Quantachrome ASiQwin. The surface areas were determined using adsorption isotherms of argon gas at 87 K. The samples were pretreated by outgassing under high vacuum at 130 °C for six hours.

Thermogravimetry and Differential Scanning calorimetry

TGA/DSC analyses were carried out with a Netzsch Jupiter STA 449 F1. The device was equipped with a SiC oven, a high-performance Heat-Flux DSC with a nanogram-resolution thermobalance and a Netzsch Typ S sensor for measurements in corrosive atmospheres. The atmosphere in the device could be set to nitrogen gas, argon gas or CO_2 gas supplied from gas bottles bought from Linde.

Acknowledgements

The TEM/SEM facilities of the Jena Center for Soft Matter (JCSM) were established with a grant from the Deutsche Forschungsgemeinschaft (DFG, German Research Foundation) and the European Fonds for Regional Development (EFRE). Mario Winkler and Joris van Slageren gratefully acknowledge financial support by the Deutsche Forschungsgemeinschaft (DFG, German Research Foundation) via Project ID 358283783 – SFB 1333. We also thank Dr Dirk Merten and Ines Kamp (ICP/OES), Antje Wermann and Steffi Ebbinghaus (XRD), Dr Seun Akintola (BET), Steffi Stumpf (SEM/EDX) and Dr Stephanie Höppener (TEM). Open Access funding enabled and organized by Projekt DEAL.

Conflict of Interest

The authors declare no conflict of interest.

Data Availability Statement

The data that support the findings of this study are available in the supplementary material of this article.

Keywords: Tochilinite · Layered hybrid materials · carbonaceous chondrites · iron sulfide · nanotubes

[1] A. R. Lennie, S. A. T. Redfern, P. F. Schofield, D. J. Vaughan, *Mineral. Mag.* **1995**, *59* (397), 677–683, https://doi.org/10.1180/minmag.1995.059.397.10.
[2] N. I. Organova, V. A. Drits, A. L. Dmitrik, *Sov. Phys. Crystallogr.* **1973**, *17* (4), 667–671.
[3] N. I. Organova, V. A. Drits, A. L. Dmitrik, *Sov. Phys. Crystallogr.* **1974**, *18* (5), 606–609.
[4] L. G. Vacher, L. Truche, F. Faure, L. Tissandier, R. Mosser-Ruck, Y. Marrocchi, *Meteorit. Planet. Sci.* **2019**, *54* (8), 1870–1889. https://doi.org/10.1111/maps.13317.
[5] Y. Muramatsu, M. Nambu, *J. Japan. Assoc. Min. Petr. Econ. Geol.* **1980**, *75* (11), 377–384.
[6] J. S. Beard, *Proc. Ocean Drill. Program* **2000**, *173*, 1–9.
[7] J. V. Milić, *J. Mater. Chem. C* **2021**, *9* (35), 11428–11443, https://doi.org/10.1039/d1tc01533h.
[8] M. Palummo, S. Postorino, C. Borghesi, G. Giorgi, *Appl. Phys. Lett.* **2021**, *119* (5), 1ENG, https://doi.org/10.1063/5.0059441.
[9] J. R. Xiao, S. H. Yang, F. Feng, H. G. Xue, S. P. Guo, *Coord. Chem. Rev.* **2017**, *347*, 23–47, https://doi.org/10.1016/j.ccr.2017.06.010.
[10] M. Valldor, B. Böhme, Y. Prots, H. Borrmann, P. Adler, W. Schnelle, Y. Watier, C. Y. Kuo, T. W. Pi, Z. Hu, C. Felser, L. H. Tjeng, *Chem. A Eur. J.* **2016**, *22*, 4626–4631, https://doi.org/10.1002/chem.201504840.
[11] Y. Peng, G. Xi, C. Zhong, L. Wang, J. Lu, X. Sun, L. Zhu, Q. Han, L. Chen, L. Shi, M. Sun, Q. Li, M. Yu, M. Yin, *Geochim. Cosmochim. Acta* **2009**, *73*, 4862–4878, https://doi.org/10.1016/j.gca.2009.05.061.
[12] M. Preiner, K. Igarashi, K. B. Muchowska, M. Yu, S. J. Varma, K. Kleinermanns, M. K. Nobu, Y. Kamagata, H. Tüysüz, J. Moran, W. F. Martin, *Nat. Ecol. Evol.* **2020**, *4* (4), 534–542, https://doi.org/10.1038/s41559-020-1125–6.

[13] C. Huber, G. Wächtershäuser, *Tetrahedron Lett.* **2003**, *44* (8), 1695–1697, https://doi.org/10.1016/S0040-4039(02)02863-0.
[14] M. J. Russell, W. Martin, *Trends Biochem. Sci.* **2004**, *29* (7), 358–363, https://doi.org/10.1016/j.tibs.2004.05.007.
[15] M. Grosch, M. T. Stiebritz, R. Bolney, M. Winkler, E. Jückstock, H. Busch, S. Peters, A. F. Siegle, J. van Slageren, M. Ribbe, Y. Hu, O. Trapp, C. Robl, W. Weigand, *ChemSystemsChem* **2022**, 4, e202200010https://doi.org/10.1002/syst.202200010.
[16] W. Heinen, A. Lauwers, *Proc. K. Ned. Akad. Wet.* **1997**, *100* (1–2), 11–25.
[17] S. V. Kozerenko, V. V. Fadeev, N. I. Chistyakova, N. N. Kolpakova, V. G. Senin, *Exp. Geosci.* **2001**, *10*, 57–58.
[18] R. Bolney, M. Grosch, M. Winkler, J. van Slageren, W. Weigand, C. Robl, *RSC Adv.* **2021**, *11* (51), 32464–32475, https://doi.org/10.1039/d1ra03705f.
[19] G. A. Kakos, T. W. Turney, T. B. Williams, *J. Solid State Chem.* **1994**, *108*, 102–111.
[20] Y. Peng, L. Xu, G. Xi, C. Zhong, J. Lu, Z. Meng, G. Li, S. Zhang, G. Zhang, Y. Qian, *Geochim. Cosmochim. Acta* **2007**, *71*, 2858–2875, https://doi.org/10.1016/j.gca.2007.03.012.
[21] Y. Peng, Y. Jing, *Earth Planet. Sci. Lett.* **2014**, *408*, 252–262, https://doi.org/10.1016/j.epsl.2014.10.020.
[22] S. V. Kozerenko, N. I. Organova, V. V. Fadeev, L. O. Magazina, N. N. Kolpakova, L. A. Kopneva, *Proc. Lunar Planet. Sci. Conf.* **1996**, *27*, 695–696.
[23] T. V. Gubaidulina, N. I. Chistyakova, V. S. Rusakov, *Bull. Russ. Acad. Sci.* **2007**, *71* (9), 1269–1272.
[24] N. I. Chistyakova, T. V. Gubaidulina, V. S. Rusakov, *Czech. J. Phys.* **2006**, *56*, 123–131.
[25] X. Zhou, C. Eckberg, B. Wilfong, S. C. Liou, H. K. Vivanco, J. Paglione, E. E. Rodriguez, *Chem. Sci.* **2017**, *8* (5), 3781–3788, https://doi.org/10.1039/c6sc05268a.
[26] V. S. Rusakov, N. I. Chistyakova, S. V. Kozerenko, V. V. Fadeev, *Proc. Lunar Planet. Sci. Conf.* **1998**, 29, 1604.
[27] J. L. Jambor, *Geol. Surv. Canada* **1976**, *76* (1B), 65–69.
[28] D. C. Harris, D. J. Vaughan, *American Mineral.* **1972**, *57*, 1037–7052.
[29] I. V. Pekov, E. V. Sereba, Y. S. Polekhovsky, S. N. Britvin, N. V. Chukanov, V. O. Yapaskurt, I. A. Bryzgalov, *Geol. Ore Deposits* **2013**, *55* (7), 567–574.
[30] C. Schröder, M. Wan, I. B. Butler, A. Tait, S. Peiffer, C. A. McCammon, *Minerals* **2020**, *10* (12), 1090.
[31] L. B. Browning, W. L. Bourcier, *Proc. Lunar Planet. Sci. Conf.* **1996**, 27, 171–172.
[32] M. E. Zolensky, *Am. Mineral.* **1986**, *71* (9–10), 1201–1209.

Manuscript received: June 22, 2022
Revised manuscript received: September 3, 2022
Accepted manuscript online: September 4, 2022

